Report
**P-20-05**
September 2020

# Water uptake through backfill block joints – evaluation of slot tests

**Mattias Åkesson**

SVENSK KÄRNBRÄNSLEHANTERING AB

SWEDISH NUCLEAR FUEL
AND WASTE MANAGEMENT CO

Box 3091, SE-169 03 Solna
Phone +46 8 459 84 00
skb.se

SVENSK KÄRNBRÄNSLEHANTERING

ISSN 1651-4416
**SKB P-20-05**
ID 1883220

September 2020

# Water uptake through backfill block joints – evaluation of slot tests

Mattias Åkesson, Svensk Kärnbränslehantering AB

# Abstract

This report presents an evaluation of tests performed with the objective to investigate the water transport and the water-uptake through slots between backfill blocks. Each test consisted of two cylindrical bentonite blocks stacked on each other and separated with spacers to set a defined slot width. Water was led into the centre of the slot with a constant inflow rate, and the evolution of the water pressure was registered, until a maximum allowed water pressure was reached. The size of the wetted zone was quantified after each test.

The first step of the evaluation was to estimate the rate of water-uptake in a bentonite block at free-swelling conditions. This was made by analysing two hydro-mechanical models implemented in the FEM program Code_Bright, with either confined (constant porosity) or free-swelling conditions. This gave support to the observation that the rate of water-uptake at free-swelling conditions appears to be two orders of magnitude higher than for confined conditions.

The second step was the development of a mathematical model which was based on the following assumptions: i) the slot is filled with water as a radial progressing front; ii) the water uptake into the bentonite is directed perpendicular to the plane of the slot and has a magnitude typical for free-swelling conditions; iii) the displacement is proportional to the cumulative water uptake; and iv) a liquid pressure builds up in the inner part of the slot once the displacement exceeds the slot thickness. The model consists of a set of differential equations which was solved numerically through programming with the MathCad software. The presented model provides a fairly realistic identification of the processes that governs the measured pressure build-up and spreading of water (i.e. free swelling, water transport through a progressing front, and closing of a gap).

# Sammanfattning

Denna rapport presenterar en utvärdering av tester som utförts i syfte att undersöka vattentransporten och vattenupptaget genom spalter mellan återfyllningsblock. Varje test bestod av två cylindriska bentonitblock, staplade på varandra och separerade med distanser vilka definierade en viss spaltbredd. Vatten leddes in i centrum av spalten med en konstant inflödeshastighet varvid utvecklingen av vattentrycket registrerades till dess att ett maximalt tillåtet vattentryck uppnåddes. Storleken på den uppfuktade zonen kvantifierades efter varje test.

Det första steget av utvärderingen var att uppskatta vattenupptagshastigheten i ett bentonitblock vid fritt svällande förhållanden. Detta utfördes genom att analysera två hydromekaniska modeller som implementerats i FEM-programmet Code_Bright, med antingen instängda förhållanden (konstant porositet) eller fritt svällande. Detta stödde observationen att vattenupptagshastigheten vid fritt svällande förhållanden tycks vara två storleksordningar högre än för instängda förhållanden.

Det andra steget var utvecklingen av en matematisk modell som baserades på följande antaganden: i) slitsen fylls med vatten som en radiell framåtskridande front; ii) vattenupptaget i bentoniten är vinkelrätt riktat mot slitsens plan och är till storlek typiskt för fritt svällande förhållanden; iii) förskjutningen är proportionell mot det kumulativa vattenupptaget; och iv) ett vätsketryck byggs upp i spaltens inre del när förskjutningen överstiger spaltens tjocklek. Modellen består av en uppsättning differentialekvationer som löstes numeriskt genom programmering med programmet MathCad. Den presenterade modellen ger en tämligen realistisk identifiering av de processer som styr den uppmätta tryckuppbyggnaden och spridningen av vatten (dvs fri svällning, vattentransport genom en framåtskridande front och stängning av ett gap).

# Contents

# 1 Background

A KBS-3V repository for spent nuclear fuel is planned to be built in Forsmark. The reference design for backfilling of the deposition tunnels is pre-compacted blocks placed in the tunnel and bentonite pellets that fill up the space between the blocks and the tunnel walls. The backfill blocks are planned to be water-unsaturated at the time they are installed, but will subsequently be hydrated with groundwater from the surrounding rock and will eventually reach a water-saturated state. This hydration may to some extent occur through the joints between the blocks, and laboratory tests were therefore performed with the objective to investigate the water transport and the water uptake through such joints.

The experimental results from these tests were reported by Sandén et al. (2020), whereas the evaluation of these tests is presented in this report. Chapter 2 gives an overview of the tests and the main results from these. An important part of the evaluation of the slot tests is a model for free swelling conditions, in particular for the used bentonite in question (Asha 2012), and the development and analysis of this model is presented in Chapter 3. A mathematical model which was developed to describe the actual slot tests is presented in Chapter 4. Finally, some concluding remarks are given in Chapter 5.

# 2 Slot tests

## 2.1 Description

The principal test design is shown in Figure 2-1. Two cylindrical bentonite blocks (diameter 280 mm and height 100 mm) were stacked on each other. A gap between the blocks was achieved by using spacers (either an O-ring or several steel pieces). Water was led into the gap from above at the center of the blocks. The applied inflow rate was kept constant by using a peristaltic pump and the water pressure was registered during the test time. Three displacement sensors registered the position of the upper block. When reaching a defined maximum allowed water pressure, the test was terminated and photo documented. The tests were made using different inflow rates (1, 5 and 10 ml/min), different slot widths (0.5, 1, 1.5, 2, 3 and 5 mm) and different maximum allowed water pressure (10, 40 and 100 kPa).

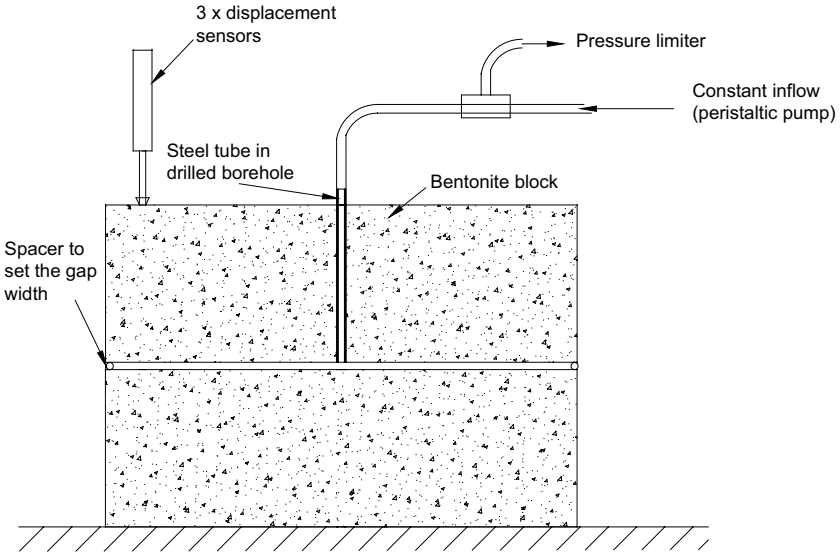


***Figure 2-1.*** *Sketch showing the principle test layout.*

## 2.2 Main results

A complete presentation of the test results is given by Sandén et al. (2020). In general, the test results show that an increased flow rate tends to increase the level of random behaviour regarding the pressure evolution and the wetting pattern observed at the termination of each test. *The focus of the evaluation of the slot tests was therefore given to the tests with the lowest flow rate: i.e. 1 ml/min*. Each test gave two types of results: i) the pressure evolution (Figure 2-2), and ii) the size (diameter) of the wetted zone (Figure 2-3).

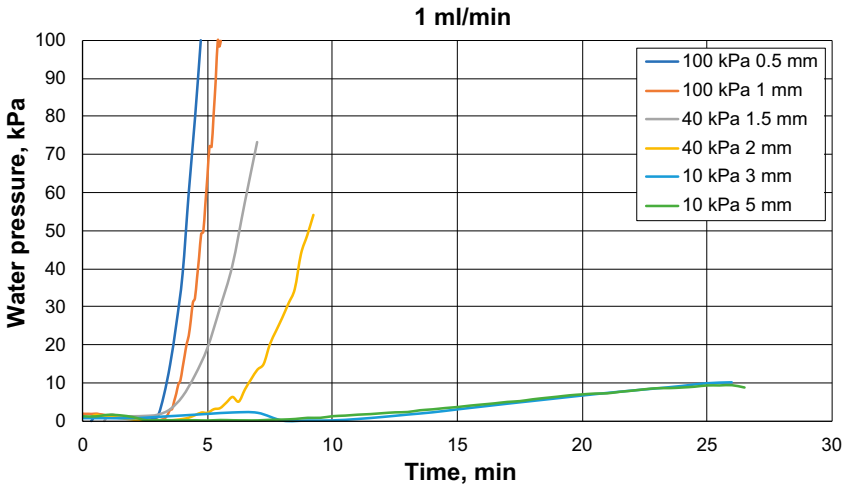


***Figure 2-2.*** *Pressure evolution of slot tests. The absence of any pressure increase during the first 3 minutes can be noted.*

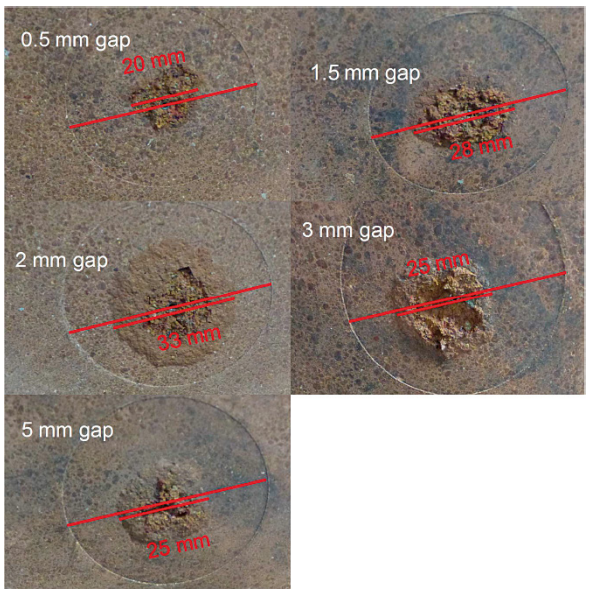


***Figure 2-3.*** *Size of wetted zone. The diameters were evaluated by comparing the widths of the wetted zone with the markings from the block compaction.*

## 2.3 Basic evaluation

Information about the extent of water uptake can be obtained by comparing the volume of supplied water during each test period with the size of the wetted zone. The diameter of a water-filled slot for a situation *without water uptake* can be calculated as:

$$Q \cdot t = d \cdot \pi \cdot \left(\frac{D_s}{2}\right)^2 \qquad D_s = \sqrt{\frac{4 \cdot Q \cdot t}{d \cdot \pi}} \tag{2-1}$$

where Q is the flow rate, t is the test duration, d is the width of the slot and $D_s$ is the diameter of the slot filling. Data from the six tests with 1 ml/min flow rate is compiled in Table 2-1. The extent of the water uptake can be estimated by squaring the ratio between the measured and the calculated diameter: $1-(D_m/D_s)^2$. This indicates that *more than 80 % of the supplied water was taken up by the bentonite*.

**Table 2-1. Compilation of performed tests.**

| Test no | Flow rate (ml/min) | Slot width (mm) | Time (min) | Diameter measured $D_m$ (mm) | Diameter slot filling $D_s$ (mm) | $1-(D_m/D_s)^2$ (-) |
|---|---|---|---|---|---|---|
| 1 | 1 | 0.5 | 5.2 | 20 | 116 | 0.97 |
| 2 | 1 | 1 | 5.9 | n.d. | 89 | |
| 3 | 1 | 1.5 | 7.0 | 28 | 77 | 0.87 |
| 4 | 1 | 2 | 9.2 | 33 | 77 | 0.82 |
| 5 | 1 | 3 | 26 | 25 | 105 | 0.94 |
| 6 | 1 | 5 | 26 | 25 | 82 | 0.91 |

To assess the water uptake capacity, the test setup with water available in the slot can be viewed as diffusion process in a semi-infinite media. Such a description would however be based on a simplification that the porosity is constant. The following expression would thereby describe the distribution of the saturation degree (S) as a function of the distance (x) from the slot, and at time t (Crank 1975, p 32):

$$S(x,t) = 1 + (S_0 - 1) \cdot \mathrm{erf}\left(\frac{x}{\sqrt{4 \cdot D \cdot t}}\right) \tag{2-2}$$

where $S_0$ is the initial saturation degree and D is the moisture diffusivity. The volumetric flux (q) at the boundary (x = 0) is given by the porosity (n), the diffusivity and the saturation gradient at the boundary:

$$q_{x=0}(t) = -n \cdot D \cdot \left.\frac{\partial S}{\partial x}\right|_{x=0} = n \cdot (1 - S_0) \cdot \sqrt{\frac{D}{\pi \cdot t}} \tag{2-3}$$

A water uptake volume (V) could thereby be calculated as the product of an boundary area (A) and the time integral of q, times 2 (two blocks facing the slot):

$$V(t) = 2 \cdot A \cdot \int_0^t q_{x=0}(\tau)\, d\tau = 4 \cdot A \cdot n \cdot (1 - S_0) \cdot \sqrt{\frac{D \cdot t}{\pi}} \tag{2-4}$$

The following example gives an indication of the magnitude of the water uptake capacity that follows from such a description. Assuming a boundary area of 0.002 $m^2$ (i.e. a circle with diameter of 0.05 m), a porosity of 0.4 (-), an initial saturation of 0.8 (-), a moisture diffusivity of $6 \times 10^{-10}$ $m^2/s$ (which is a relatively high value), and a time period of 20 min, this would give a volume of only 0.3 ml. This example thus indicates that the water uptake capacity that follows from an approach with constant porosity *will underestimate the actual water uptake with approximately two orders of magnitude*.

## 2.4 Outline of analysis

Based on the findings from the basic evaluation presented above, the main evaluation of the slot tests was performed in two steps:

i) The rate of water uptake at free swelling conditions was analysed. This part also involved the parameter value adoption for the bentonite blocks in question.

ii) By using the description of water uptake for free swelling conditions a mathematical model of the slot tests was development and analysed.

# 3 Model of free swelling

## 3.1 Introduction

This chapter consists of three section. The first section describes the parameter value adoption for the bentonite blocks. The second section describes two Code_Bright models, with either confined or free swelling conditions. An evaluation of these models and implication of the results for the evaluation of the slot tests are presented in the third section.

## 3.2 Asha 2012 material

There is generally very little available information about the bentonite in the block used in the slot tests (i.e. Asha 2012).

Regarding measurement of *water retention properties*, there has been no dedicated tests (e.g. jar tests) with Asha 2012. Johannesson et al. (2008) presents a water retention curve obtained for Asha 230B, but this appears to be a material which is significantly different than the material used here. Data obtained for MX-80 has therefore been used as a proxy in this evaluation. The relevance of this approach is supported by the results from tests with water transport in pellets-filled slots, analysed within EBS Taskforce (Åkesson 2020).

Regarding *water uptake tests,* there has been no tests performed with Asha 2012. Tests results for Asha 230B presented by Johannesson et al. (2008) and evaluated by Sellin et al. (2017) showed a moisture diffusivity value of approximately $6 \times 10^{-10}$ m$^2$/s. Since this value is relatively high in comparison to data for MX-80, it is used as a proxi for high density confined conditions, in spite of the fact that it was obtained for a very different material.

Regarding *hydraulic conductivity,* there are quite a large set of data for Asha 2012, which was presented by Sandén et al. (2014). No measurement has however been performed at a dry density level of 1 720 kg/m$^3$ used for the block in these tests.

## 3.3 Code_Bright models

Two models, for confined and free swelling conditions respectively, were developed with Code_Bright (v4). A 1D plane geometry with a length of 0.02 m and width of 0.0002 m were used for both models (Figure 3-1). Each geometry was discretized in 100 elements.

The initial porosity for both models, 0.411, was based on a dry density of 1 720 kg/m$^3$ and a solid density of 2 920 kg/m$^3$. The initial degree of saturation used for both models, 0.837, was based on a water content of 20 %. For the free swelling model an initial stress of 10 kPa was applied. In both models, the temperature was 20 ºC and the gas pressure was 0.1 MPa.

A hydraulic boundary condition with a constant liquid pressure of 0.1 MPa ($\gamma$ = 10) was applied in both models on the left side (Figure 3-1). For the free swelling model, mechanical boundary conditions with roller boundary at the left side, whereas stress boundaries (with 10 KPa) were applied at the remaining three sides.

Both models simulated the evolution during a time period of 20 minutes.

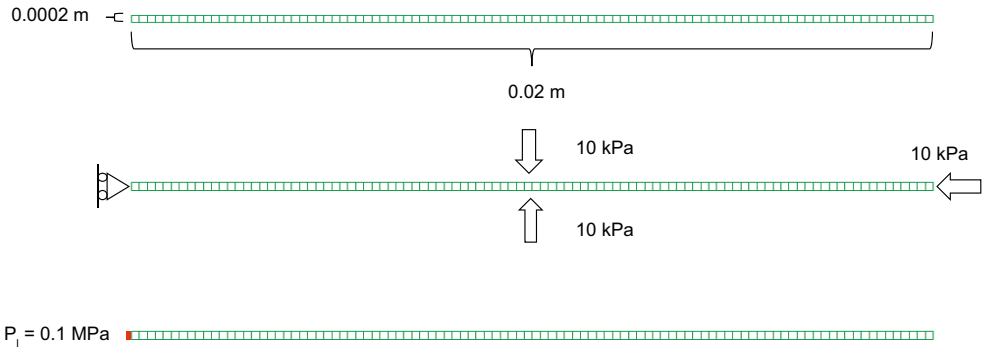


***Figure 3-1.*** *Model geometry (upper), mechanical BC (middle) and hydraulic BC (lower).*

### *Parameter value adoption*

Two *water retention curves* were adopted for the two Code_Bright models. In both cases, a relation between the clay potential and the void ratio, here denoted $\Psi_L(e)$ and originally adopted by Åkesson et al. (2010), was used as a target. For the initial conditions, this meant that the initial suction value was 18.7 MPa.

For *confined conditions*, a square law type curve was employed:

$$S_l(s) = \frac{1}{\sqrt{1 + s/P_0}} \tag{3-1}$$

where $S_l$ is the degree of saturation, s is suction and $P_0$ is a parameter. In order to obtain the correct initial conditions, the $P_0$ value was set to 43.7 MPa (Figure 3-2, left). A useful property of this type of curve is that it together with a cubic relative permeability law corresponds to constant diffusivity value (see below).

For *free swelling conditions*, a van Genuchten type curve was employed:

$$S_l(s) = \left(1 + \left(\frac{s}{P_0}\right)^{\frac{1}{1-\lambda}}\right)^{-\lambda} \tag{3-2}$$

where $P_0$ and $\lambda$ are parameters. The adoption of this curve followed an approach proposed by Sandén et al. (2008) according to which the air-filled void ratio ($e_M = V_g/V_s$) is assumed to be constant during swelling:

$$S_l(s) = \frac{e_m(s)}{e_m(s) + e_M} = \left(1 + \frac{e_M}{e_m(s)}\right)^{-1} \tag{3-3}$$

where $e_m(s)$ is the water-filled void ratio as a function of the suction. This function was described as the inverse function of $\Psi_L(e)$ mentioned above, whereas $e_M$ was calculated as the initial value of $e\cdot(1-S_l)$, i.e. 0.114. A van Genuchten type curve was adopted in order to resemble this curve (Figure 3-2, right), with the following parameter values: $P_0 = 0.039$ MPa and $\lambda = 0.028$.

Swelling is described with the *swelling modulus* $\kappa_s$ in the Barcelona Basic Model (BBM). From the definition of this parameter follows a relation between the void ratio and the suction:

$$e(s) = e_{init} - \int_{s_{init}}^{s} \frac{\kappa_s}{s' + 0.1} ds' \tag{3-4}$$

The approach with a constant air-filled void ratio mentioned above implies the following simple relation between the void ratio and the suction:

$$e(s) = e_m(s) + e_M \tag{3-5}$$

The $\kappa_s$-value was calibrated to 0.21 so that the swelling behaviour of BBM resembles this curve (Figure 3-3). Since the swelling in the out-of-plane direction of the model was zero, the actual $\kappa_s$-value was increased with a factor of 1.5 to 0.32. The remaining elastic parameters were set to avoid any influence on the results: $\kappa_i = 1$; $K_{min} = 0.1$ MPa, $\nu = 0.2$. The yield surface parameters were set so that plastic conditions were never reached.

Finally, a relation between the *intrinsic permeability* (k) and the porosity was adopted. For the *relative permeability* a cubic law ($k_r = S_l^3$) was assumed for both the confined and the free swelling model. The following equation gives a relation between the k-value, the relative permeability relation, the derivative of the retention curve, the porosity, the viscosity and the moisture diffusivity:

$$D = -\frac{k \cdot k_r(S_l)}{n \cdot \mu}\frac{ds}{dS_l} \tag{3-6}$$

The derivative of the square law retention curve can be evaluated as: $ds/dS_l = -2P_0/S_l^3$. From this follows that the k-value can be evaluated as:

$$k = \frac{n \cdot \mu \cdot D}{2P_0} \tag{3-7}$$

For the initial porosity ($n_0$) of 0.411 and a diffusivity value of $6 \times 10^{-10}$ m$^2$/s this gives a k-value of $2.8 \times 10^{-21}$ m$^2$. This was used as a reference value ($k_0$) for the porosity dependence implemented in Code_Bright as:

$$k(n) = k_0 \cdot exp[b \cdot (n - n_0)] \tag{3-8}$$

where b is a parameter. Together with empirical data on the hydraulic conductivity for different dry densities, this parameter was adopted to a value of 40 (Figure 3-4).

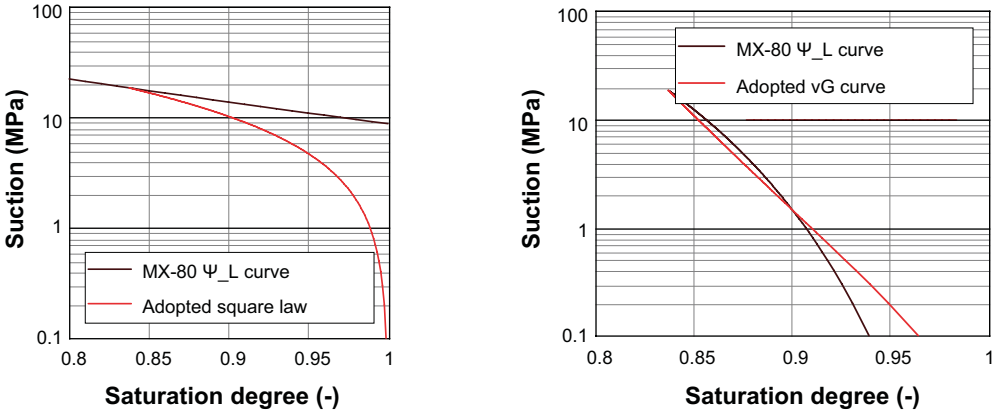


***Figure 3-2.*** *Water retention curves; confined conditions (left) and free swelling conditions (right).*

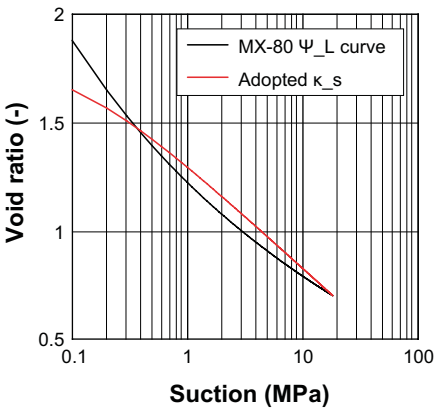


***Figure 3-3.*** *Relation between void ratio and suction.*

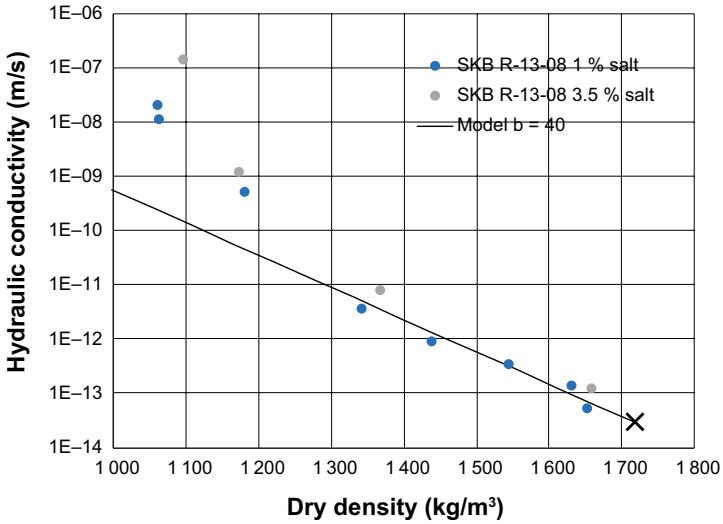


***Figure 3-4.*** *Hydraulic conductivity versus dry density.*

## 3.4 Evaluation

The *confined model* was analysed regarding the saturation profile at the end of the simulation and regarding the evolution of the volumetric flux at the hydraulic boundary. Both these results demonstrated a good agreement with the analytical description as described by Equation (2-2) and (2-3), see Figure 3-5.

The *free swelling model* was first evaluated in order to verify that the adopted retention curve and the $\kappa_s$-value together resulted in a relation between water content and RH which was consistent with experimental data for MX-80. This was made for model results for all nodes for four different times (2, 5, 10 and 20 min). The $\Psi_L$ ($e$) relation, mentioned above, was used to represent empirical data, for which suction values were converted to RH values (Kelvin´s equation), and void ratio values were converted to water contents ($w = e \cdot \rho_w/\rho_s$). The comparison is shown in Figure 3-6 (left) and the agreement is apparently fairly accurate. A corresponding comparison was made for the relation between the void ratio and the suction; both for evaluated model results and for the analytical expression in Equation (3-4) (Figure 3-6, right). These comparisons thus indicate that the *behaviour of the model is in general agreement with bentonite behaviour* according to current knowledge.

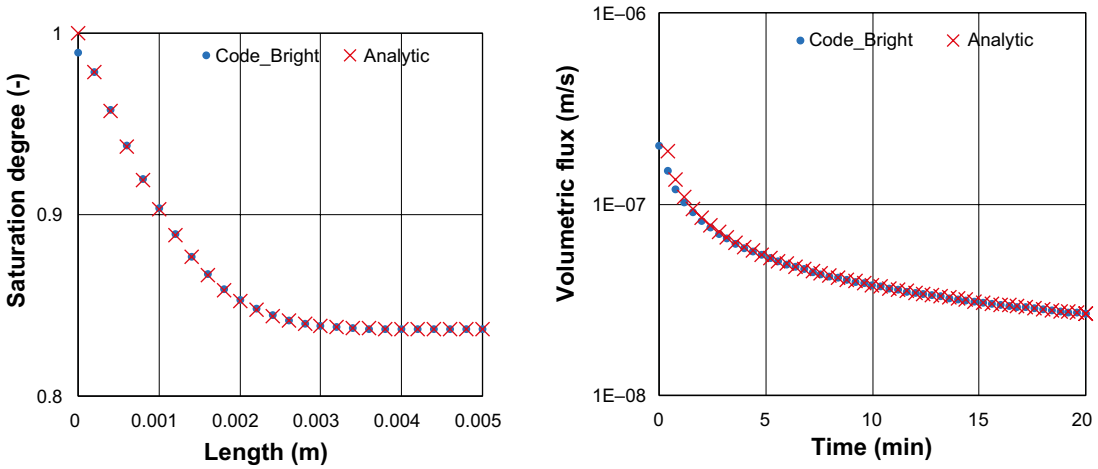


***Figure 3-5.*** *Confined conditions. Saturation profile for 20 minute (left) and inflow flux evolution (right). Numerical and analytical results.*

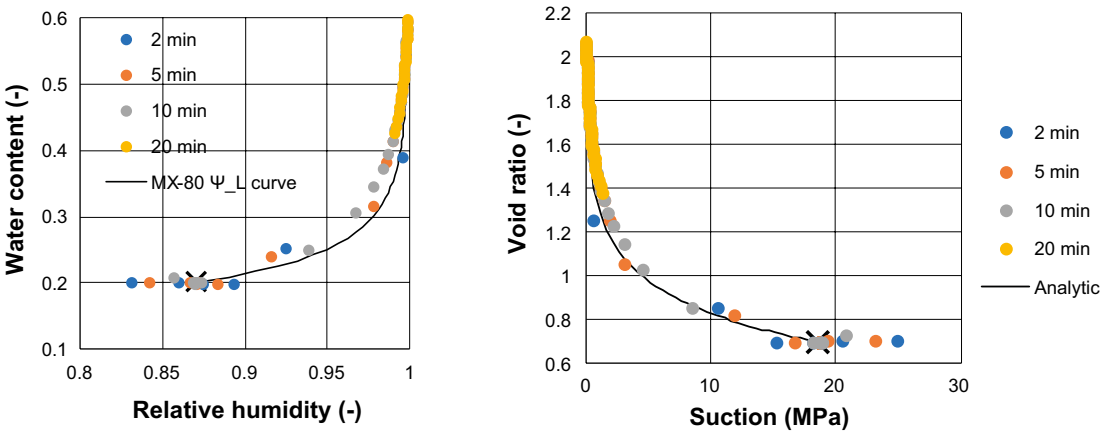


***Figure 3-6.*** *Free swelling. Water content versus RH (left), void ratio versus suction (right) for different times.*

The quite dramatic evolution of the free swelling model is illustrated in Figure 3-7. The left graph shows porosity profiles for different times and shows the progress of a front with significantly increased porosity values. The right graph shows the evolution of the volumetric flux at the hydraulic boundary together with a fitted analytical description as described by Equation (2-3). In contrast to the empirical diffusivity value evaluated for confined conditions, the calibrated value was found to be $4 \times 10^{-6}$ m$^2$/s. Given that the flux is proportional to the square root of the diffusivity, this results appears to be quite consistent with the main finding from the basic evaluation in Section 2.3.

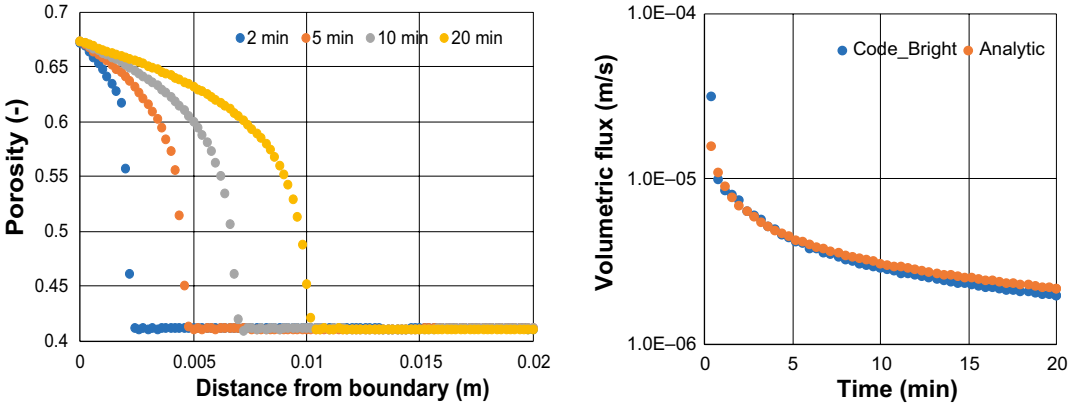


***Figure 3-7.*** *Free swelling. Porosity profiles for different times (left). Inflow flux evolution (right). Numerical results and fitted diffusivity.*

# 4 Mathematical model of slot test

## 4.1 General outline

This chapter presents a mathematical model which was developed with the goal to simulate the slot tests.

The definition of the different parts of the model is first described: i) the filling of the slot as a progressing water filling front; ii) the water uptake into the bentonite perpendicular to the plane of the slot (rate of water uptake set from diffusivity value adopted in Section 3.4); iii) the displacement assumed to be proportional to the cumulative water uptake; and iv) the build-up of a liquid pressure in the inner part of the slot once the displacement exceeds the slot thickness. The model, consisting of a set of differential equations was solved numerically (by simple Euler forward) through programming in the MathCad software. Finally, the model results were compared with experimental data, especially regarding the build-up of water pressure and the area of the wetted zone at the time of termination of the tests.

## 4.2 Model definition

The model was based on a set of assumptions.

i) The slot is filled radially from the centre as a progressing front (see Figure 4-1).

ii) A perpendicular water uptake into the bentonite at radius r starts once the front has passed this radius. This volumetric flux is derived from Equation (2-3):

$$q(r,t) = n \cdot (1 - S_0) \cdot \sqrt{\frac{D}{\pi \cdot (t - t_f(r))}} \tag{4-1}$$

where $t_f(r)$ denote the time when the front has passed the radius r (Figure 4-1, upper).

iii) The water uptake ($Q^{ut}$) within a circle with radius r is thereby give as (Figure 4-1, left):

$$Q^{ut}(r,t) = \int_0^r 2\pi r' \cdot q[r',t]\, dr' \tag{4-2}$$

iv) The difference between the inflow rate (Q) and the total water uptake determines the rate by which the filling front at radius $r_f$ progresses (Figure 4-1, upper):

$$2\pi r_f \cdot d \cdot \frac{dr_f}{dt} = Q - Q^{ut}(r_f,t) \tag{4-3}$$

v) The displacement of the bentonite surface (u) at radius r is assumed to be proportional to the cumulative water uptake:

$$u(r,t) \sim \chi \cdot \int_0^t q(r,\tau)\, d\tau = \chi \cdot 2 \cdot n \cdot (1 - S_0) \cdot \sqrt{\frac{D \cdot \left(t - t_f(r)\right)}{\pi}} \tag{4-4}$$

where $\chi$ is proportionality factor (Figure 4-1, left).

vi) The liquid pressure (P) will build up in the inner part of the slot once the displacement exceeds the slot thickness. The pressure gradient profile is determined by the distribution of the total flow rate and the zero-pressure level at the position where the displacement is equal to the thickness:

$$\frac{dP}{dr} = -\frac{\gamma}{2\pi r \cdot d \cdot K}\left(Q - Q^{ut}(r,t)\right) \tag{4-5}$$

where γ is the specific weight of water and K is the hydraulic conductivity (Figure 4-1, right).

The set of differential equation above were solved numerically through programming in the MathCad software.

The process was discretised in time with a defined time increment ($\Delta t$, and the time (t) and the radius (r) of the filling front was saved for each time step j (Figure 4-2). For each time step j, the water uptake within all inner radii ($r_i$) were calculated from Equation (4-2):

$$Q_i^{ut} = \sum_{k=0}^{i} \pi \cdot \left[r_{k+1}^2 - r_k^2\right] \cdot q\left[t_j - \frac{t_{k+1} + t_k}{2}\right] \quad (4\text{-}6)$$

In addition, the displacement at time step j and at all inner radial position ($r_i$) were simply calculated with Equation (4-4) as $u\ (t_j - t_i)$. The liquid pressure is assumed to be zero at all radial positions where the displacement is lower than the thickness of the slot (d). Inside the circle where u exceeds d, the pressure profile obtained by integration of Equation (4-5):

$$P_{i-1} = P_i + \frac{\gamma}{2\pi \cdot d \cdot K} \cdot 2 \cdot \frac{r_i - r_{i-1}}{r_i + r_{i-1}} [Q - Q_i^{ut}] \quad (4\text{-}7)$$

Finally, the radius for the subsequent time step is calculated from Equation (4-3):

$$r_{j+1} = \sqrt{r_j^2 + \frac{\Delta t \cdot \left(Q - Q_{j-1}^{ut}\right)}{\pi \cdot d}} \quad (4\text{-}8)$$

The model was run for cases with the parameters value shown in Table 4-1. The D value was taken from the results presented in Section 3.4. The K value was generally consistent with the experimental data shown in Figure 3-4 and for a dry density of 1 000 kg/m$^3$. The X value was tuned so that the calculated delay in pressure build-up resembled the experimental data. The initial time increment ($\Delta$t) was set to 0.01 s. Subsequent time increments were increase geometrically with 1.8 %. Each model simulated a time period of 40 minutes.

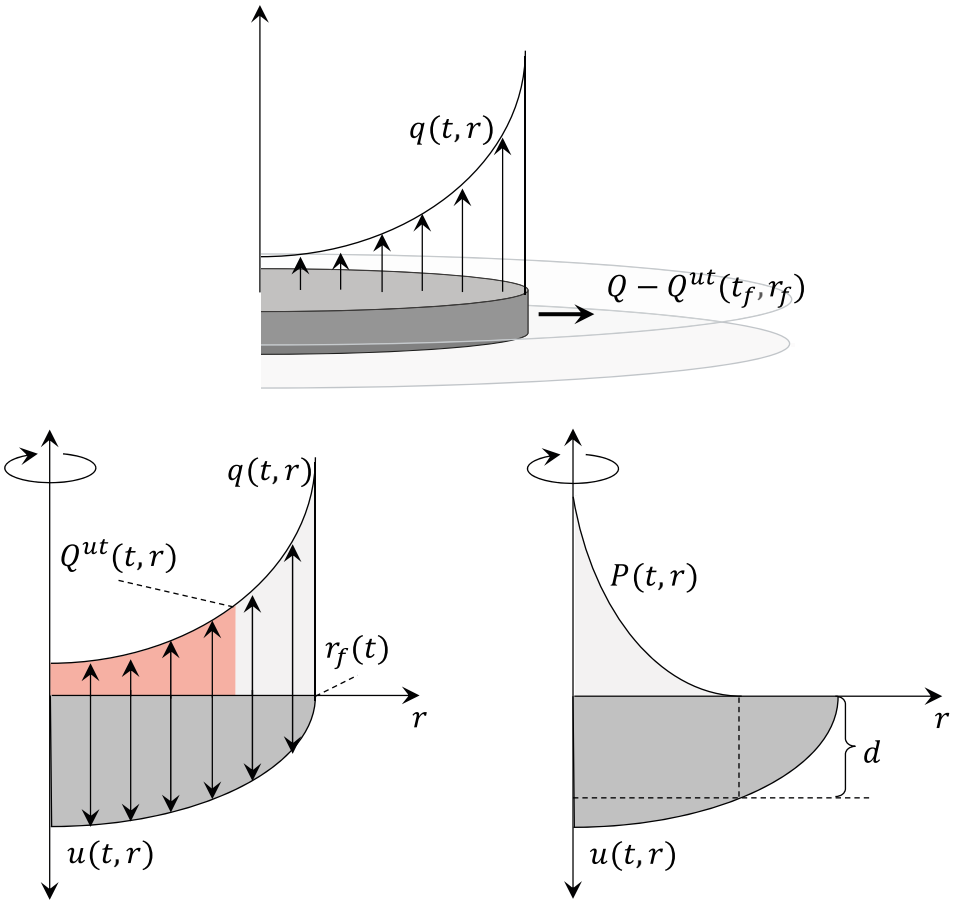


***Figure 4-1.*** *Schematic illustration of model. The progressing front and the volumetric flux (upper picture). The water uptake within a circle with radius r and the displacement (lower left). Liquid pressure profile in the inner part of the slot where the displacement exceeds the slot thickness d (lower right).*

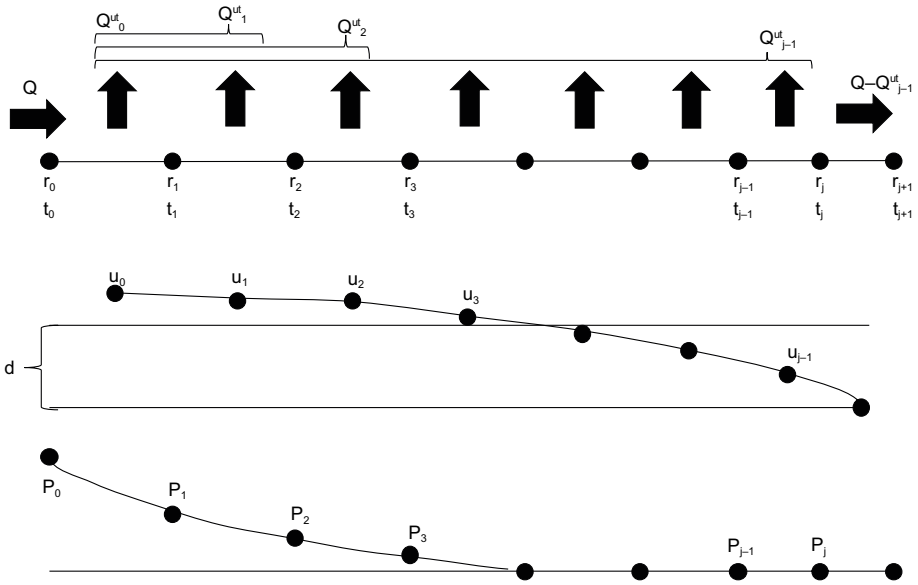


***Figure 4-2.*** *Discretization of model. Array of radius (r) and time (t), corresponding to the progress of the filling front. Quantities (water uptake $Q^{ut}$, displacement u, and pressure P) calculated each time step j.*

**Table 4-1. Parameter values used for model cases.**

| d (mm) | n (-) | $S_0$ (-) | K (m/s) | D ($m^2$/s) | Q (ml/min) | X (-) |
|---|---|---|---|---|---|---|
| 0.5, 1, 2 | 0.411 | 0.837 | $10^{-6}$ | $4 \times 10^{-6}$ | 1 | 0.15 |

Since the model only represents one of the bentonite blocks, the flow rate used in the model was *half the value* used in the experiment, and the closing of the slot occurred when the displacement equalled *half the defined slot thickness*.

## 4.3 Results

Model results for the case with a 0.5 mm slot is shown in Figure 4-3. Distributions of different variables illustrate the conditions after 40 minutes of simulation. The water uptake $Q^{ut}$ increases with the radius and almost reaches the level of the inflow rate Q at the radius of the *water filling front*. In contrast, the displacement decreases with the radius to the same point where the displacement is zero. It can be noted that the radius where the displacement is equal to half the slot thickness (i.e. 0.25 mm), i.e. the *gap closing front,* is very close to the water filling front. The liquid pressure also decreases with radius and reaches zero at the gap closing front. The pressure at a radius of 2 mm is marked and represents a pressure level that can be measured in the water supply tube. In addition, evolutions of three variables are also shown in Figure 4-3: the progressing water filling front, the gap closing front and the liquid pressure evolution at a radius of 2 mm. It can be noted that the delay in the build-up of liquid pressure corresponds to the delay of the progress of the gap closing front.

Evolutions of the liquid pressure (at 2 mm radius) and the progress of the water filling fronts are shown for the three model cases in Figure 4-4. This graph can be compared with the measured pressure evolutions in Figure 2-2, and with the measured sizes of the wetted zones shown in Figure 2-3. It can be noted that the calculated pressure evolution resembles the measured results to some extent, especially the rapid increase after some delay up to ~100 kPa for the case with d = 0.5 mm. In addition, the calculated pressure build-up with the larger slot widths are also significantly slower than for 0.5 mm. The radiuses of the water filling fronts are all in the order of 20 mm for the times which correspond to the termination of the tests. This is however almost twice as high as the measured sizes of the wetted zones.

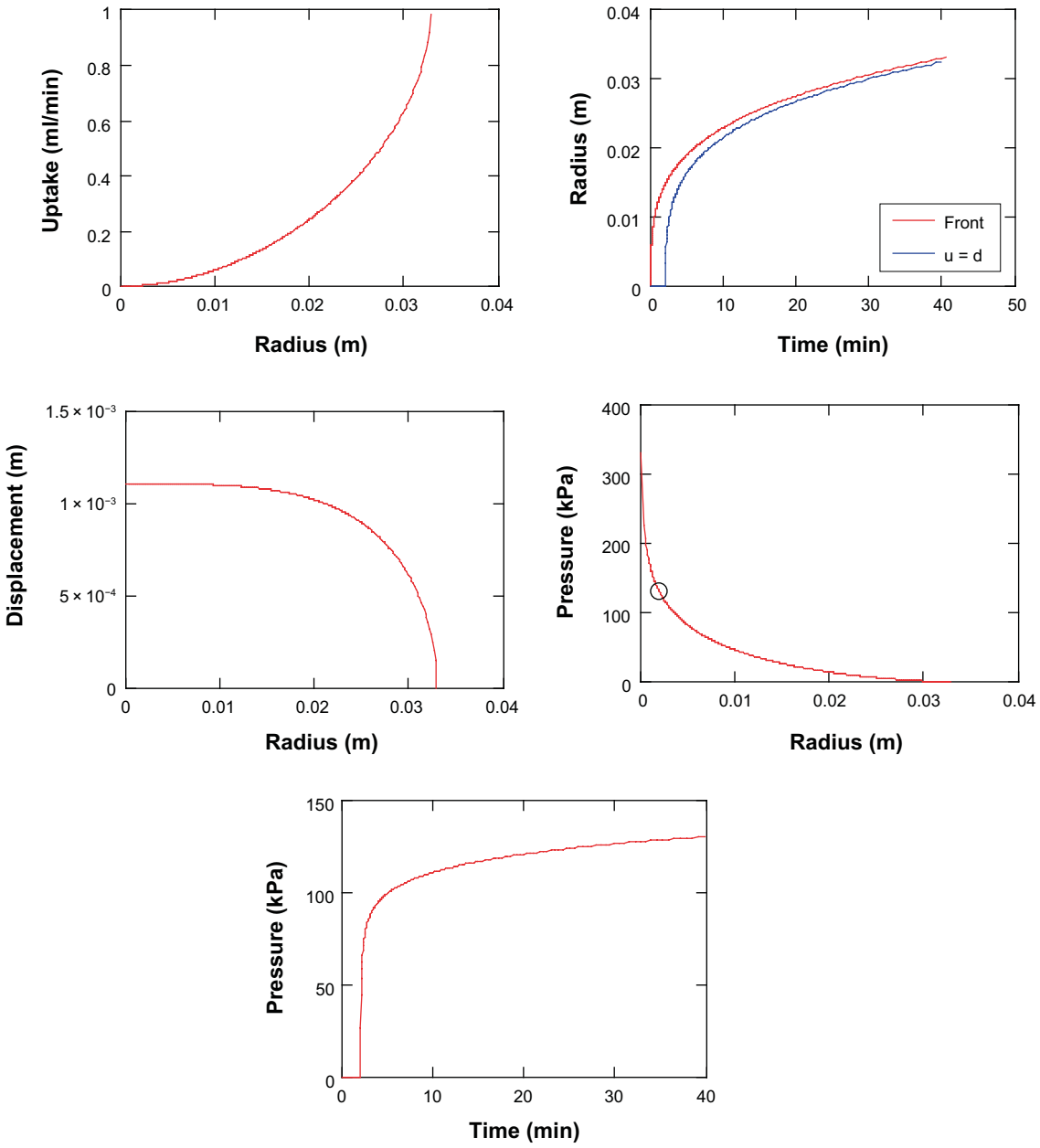


***Figure 4-3.*** *Model results for test case with d = 0.5 mm and Q = 1 ml/min.*

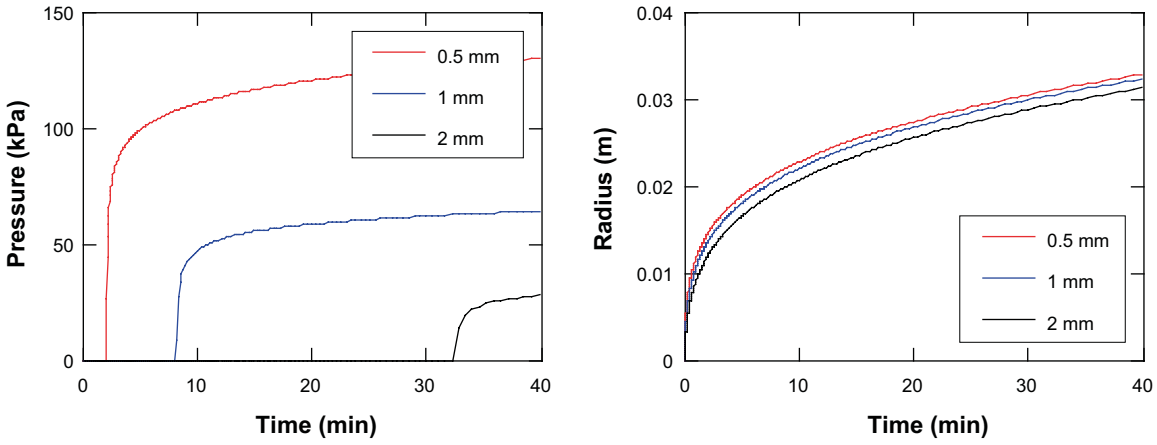


***Figure 4-4.*** *Model results for test cases with different d-values and Q = 1 ml/min.*

# 5 Concluding remarks

The presented model provides a fairy realistic identification of the processes that govern the measured pressure build-up and spreading of water (i.e. free swelling, water transport through a progressing front, and closing of a gap) even though the model results are different than the experimental data in several aspects. Irregular pressure evolution and wetting pattern observed at higher flow rates also indicate that the overall behaviour may be governed by even more complex processes, e.g. through piping and erosion.

The largest weakness of the presented model is probably the representation of the water uptake as a one-dimensional diffusion processes perpendicular to the plane of the slot. It can be expected that this approach underestimates the overall rate of water uptake. A second weakness of the model is the general lack of data for the studied bentonite material from independent tests, especially regarding retention properties.

Finally, it should be stressed that the very high diffusivity value derived from the Code_Bright model in Chapter 3 can only be representative for water uptake at free swelling conditions. To the authors knowledge, this is the first time this type of evaluation has been performed. This process should therefore be analysed in more detail.

# References

SKB's (Svensk Kärnbränslehantering AB) publications can be found at www.skb.com/publications.

**Crank J, 1975.** The mathematics of diffusion. 2nd ed. Oxford: Oxford University Press.

**Johannesson L-E, Sandén T, Dueck A, 2008.** Deep repository – engineered barrier system. Wetting and homogenization processes in backfill materials. Laboratory tests for evaluating modeling parameters. SKB R-08-136, Svensk Kärnbränslehantering AB.

**Sandén T, Börgesson L, Dueck A, Goudarzi R, Lönnqvist M, Nilsson U, Åkesson M, 2008.** KBS-3H. Description of buffer tests in 2005–2007. Results of laboratory tests. SKB R-08-40, Svensk Kärnbränslehantering AB.

**Sandén T, Olsson S, Andersson L, Dueck A, Jensen V, Hansen E, Johnsson A, 2014.** Investigation of backfill candidate materials. SKB R-13-08, Svensk Kärnbränslehantering AB.

**Sandén T, Kristensson O, Lönnqvist M, Börgesson L, Nilsson U, Goudarzi R, 2020.** Buffer swelling. Laboratory tests and modelling. SKB TR-20-04, Svensk Kärnbränslehantering AB.

**Sellin P (ed), Åkesson M, Kristensson O, Malmberg D, Börgesson L, Birgersson M, Dueck A, Karnland O, Hernelind J, 2017.** Long re-saturation phase of a final repository. Additional supplementary information. SKB TR-17-15, Svensk Kärnbränslehantering AB.

**Åkesson M, Börgesson L, Kristensson O, 2010.** SR-Site data report. THM modelling of buffer, backfill and other system components. SKB TR-10-44, Svensk Kärnbränslehantering AB.

**Åkesson M, 2020.** EBS TF – THM modelling. Water transport in pellets-filled slots. Modelling of test cases A and C. SKB P-20-19, Svensk Kärnbränslehantering AB.

Arkitektkopia AB, Bromma, 2020

SKB is responsible for managing spent nuclear fuel and radioactive waste produced by the Swedish nuclear power plants such that man and the environment are protected in the near and distant future.

**skb.se**